Journal of Porous Materials
https://doi.org/10.1007/s10934-018-0645-9

Iron-doped mesoporous silica, Fe-MCM-41, as an active Lewis acid catalyst for acidolysis of benzyl chloride with fatty acid

Zhuxiu Zhang[1] · Mengnan Hu[1] · Qiumin Mei[1] · Jihai Tang[1,2] · Zhaoyang Fei[1] · Xian Chen[1] · Qing Liu[1] · Mifen Cui[1] · Xu Qiao[1,2]

Abstract
Iron-doped mesoporous silica, Fe-MCM-41, with different concentrations of Lewis acidity have been prepared by the hydrothermal method. Physicochemical properties of all Fe-MCM-41 samples were obtained via HRTEM, PXRD and N_2 sorption characterization. The surface acidities were tested by NH_3-TPD. The catalytic activity of all Fe-MCM-41 materials were evaluated in the acidolysis reaction of benzyl chloride with various fatty acids. The corresponding benzaldehyde and acyl chloride product were synthesized in good conversion and high atom efficiency over the catalyst with the highest Fe content.

Keywords Fe-MCM-41 · Lewis acid catalyst · Acidolysis · Coproduction

1 Introduction

Lewis acids such as metal salts and simple metal complexes are important catalysts in the current industrial process [1–3]. However, they tend to decompose or deactivate with the presence of water. Moreover, it is necessary to use excess amount of such catalysts for the reaction, which raises problem in the post-reaction purification process and generate difficulty in recycling catalysts [4]. Therefore, many efforts have been devoted to develop heterogeneous catalysts with Lewis acidity. Different types of porous materials including zeolite [3], metal–organic frameworks [5] and ordered mesoporous silica [6] have been explored as active Lewis catalysts. Zeolites are among the most extensively studied heterogeneous catalysts with Lewis acidity. For example, the titanium silicate was shown to exhibit only Lewis acidity other than Brønsted acidity [7]. Nevertheless, zeolites normally have only micropores that are not beneficial for the mass transfer of substrates during the catalytic reactions. It is easy to fabricate metal–organic framework with various Lewis acidity since the structure is composed of metals/metal clusters linked by organic ligands. Despite Cr-based MOFs (e.g. MIL-101 [8] and MIL-53 [9]) and Zr-based MOFs (e.g. MOF-808 [10] and UiO-66 [11]), most of MOFs suffer the stability problems. Thus, the silica-based porous materials such as MCM-41 [12], SBA-15 [13] and KIT-6 [14] with fine-tunable pore size and pore chemistry have been a topical interest in the field of catalytic materials.

Due to the regular structure, sufficient one-dimensional channel and high surface area, MCM-41 mesoporous silica is the desirable platform for the design of functional catalysts. They have shown high catalytic activity in varieties of organic transformations, such as chemical fixation of CO_2 [12], Fenton oxidation [15], and hydrogenation [16]. Pure MCM-41 failed to exhibit sufficient surface acidity and catalytic properties, but there are a handful of approaches for the fabrication of Lewis acidity in MCM-41. For example, the isomorphous substitution of silicon with metal cations such as Al^{3+}, Fe^{3+}, Ce^{4+} and Zr^{4+} can render MCM-41 with strong Lewis acidity [17–20]. The incorporation of the trivalent metal cation is of particular interest because it can significantly affect the acid strength and catalytic performance. For example, Fe-doped MCM-41, Fe-MCM-41, with high concentration of Fe is essential

✉ Jihai Tang
jhtang@njtech.edu.cn

✉ Mifen Cui
mfcui@njtech.edu.cn

[1] State Key Laboratory of Materials-Oriented Chemical Engineering, College of Chemical Engineering, Nanjing Tech University, No. 5 Xinmofan Road, Nanjing 210009, China

[2] Jiangsu National Synergetic Innovation Centre for Advanced Materials (SICAM), Nanjing Tech University, No. 5 Xinmofan Road, Nanjing 210009, China

Published online: 24 July 2018

for the hydroxylation of phenol with dihydroxybenzene selectivity of 78.3% [21]. It also shows exceptional catalytic activity in the ozonation of *p*-chlorobenzoic acid [17] and Mukaiyama aldol reaction [22].

The acidolysis of benzyl chloride with fatty acid has recently attracted considerable attentions because it realizes the coproduction of benzaldehyde and acyl chloride. The traditional approach for the respective production of benzaldehyde and acyl chloride will form larger amount of either HCl or SO_2 as byproducts, of which the atom efficiency of the reaction is < 60%. In contrast, the atom efficiency of coproduction approach is 86% with only highly reduced amount of HCl as byproduct. To date, Lewis acids such as $FeCl_3$, $AlCl_3$ and $SnCl_4$ have been used as the homogeneous catalysts for this coproduction process, but this is not yet the case for heterogeneous catalysts [23]. It occurs to us that Fe-MCM-41 can serve as the heterogeneous catalyst other than the homogeneous counterparts for this reaction. Herein, we address the synthesis of Fe-MCM-41 with different Fe contents, and we study the effect of Fe contents on catalytic activity in the context of acidolysis of benzyl chloride with fatty acids.

2 Experimental section

2.1 Catalyst preparation

The preparation procedure of Fe-MCM-41 was similar to that reported in the literatures [24]. The cationic surfactant cetyltrimethylammonium bromide (CTAB) was used as the structure directing agent and tetraethyl orthosilicate (TEOS) along with ferric chloride as the silicon and iron sources, respectively. The typical preparation of Fe-MCM-41 was conducted as follows: 3.82 g of CTAB and 1.71 g of $FeCl_3{\cdot}6H_2O$ were dissolved in 90 g of deionized water. The resulting solution was stirred for 30 min and 27% $NH_3{\cdot}H_2O$ was added into the solution until the pH reached 9–10. Then, 20 g of TEOS was added dropwise into the solution. The resulting sol was placed into an autoclave and heated at 110 °C under static condition for 5 days. After cooling to room temperature, the solid was washed with deionized water and air-dried at 110 °C. To remove the template CTAB, the product was subsequently calcined in air at 550 °C for 6 h. The resulting white power was designated as *x*Fe-MCM-41, where *x* is the theoretical molar ratio of Fe to Si in the solids, and $x = 0$, 2, 4 denote the molar ratio of Fe to Si is 0, 2 and 4%, respectively. For comparison, pure silica MCM-41 with the same molar composition (excluding ferric chloride) was also prepared and used as a catalyst in the reaction.

2.2 Catalyst characterization

The low angle X-ray diffraction patterns were collected on a Smartlab TM 9KW. The diffraction data were recorded in the 2θ range of 1.5°–8° at an interval of 0.02° with a scanning rate of 1°/min.

N_2 sorption isotherms of the samples were obtained on a BETSORP-II analyzer at − 196 °C. Before experiment, the samples were pretreated under vacuum at 200 °C for 3 h. The specific surface areas of the samples were calculated using the BET method. The pore size distribution and pore volume were determined with BJH equations using adsorption data.

Fourier transform infrared (FT-IR) spectra of the samples were recorded with Thermo Nicolet NEXUS spectrometer in the range of wave numbers 400–4000 cm^{-1}. The iron contents of the samples were analyzed using ICP-AES after dissolving completely in the hydrofluoric acid. UV–Vis diffuse reflectance spectra were measured with a Perkin–Elmer Lambda 35 spectrometer equipped with a Praying-Mantis diffuse reflectance attachment.

The temperature-programmed desorption of ammonia (NH_3-TPD) measurements were carried out using Micromeritics Autochem 2920 instrument. Prior to analysis, the samples were degassed at 500 °C in the vacuum. The sorption of NH_3 was carried out at 100 °C, and then the gaseous and weakly adsorbed NH_3 was purged with He. NH_3-TPD was then performed in He flow by raising the temperature to 600 °C with a heating rate of 10 °C/min.

2.3 Catalyst test for coproduction of benzaldehyde and pivaloyl chloride

The coproduction of benzaldehyde and pivaloyl chloride was carried out in a 100 mL three necked round bottom flask with a sampling port, thermometer and reflex condenser. In a standard reaction, a reaction flask was charged with 15.5 g of pivalic acid, 39 g of benzyl chloride (1:1.6 molar ratio) and 0.022 g of catalyst. Then the reaction vessel was heated to 110 °C, and maintained for 1 h.

All collected samples were analysed by gas chromatography (SP-6800A) equipped with a capillary 30 m × 0.32 mm × 0.25 μm SE-54 column and a flame ionization detector (FID), in which ethylbenzene was used as an internal standard. The initial temperature was 110 °C, the temperature ramp rate was 30 °C/min, and the final temperature was 200 °C. The temperature of the FID detector and gasification chamber was both 220 °C. The performance of the catalyst was evaluated quantitatively using the conversion of pivalic acid and selectivity of benzaldehyde and pivaloyl chloride.

The detailed formulas of conversion, selectivity and yield of the acidolysis of benzyl chloride with fatty acid are as follows:

$$X_{FA} = 1 - \frac{\omega_{FA} m_0}{M_{FA} n_{FA0}} \quad (1)$$

$$S_i = \frac{\omega_i m_0 / M_i}{n_{FA0} - m_0 \omega_{FA/M_{FA}}} \quad (2)$$

$$Y_i = X_{FA} S_i \quad (3)$$

X_{FA} is the conversion of fatty acid. S_i is the selectivity of benzaldehyde or pivaloyl chloride. Y_i is the yield of benzaldehyde or pivaloyl chloride. m_0 is the mass of the reaction mixture. ω_{FA} and ω_i are the mass content of fatty acid and benzaldehyde or pivaloyl chloride respectively. M_{FA} and M_i are the molar mass of fatty acid and benzaldehyde or pivaloyl chloride respectively. n_{FA0} is the molar amount of fatty acid added to the reaction.

3 Result and discussion

3.1 Catalyst characterization

N_2 sorption isotherms of the prepared Fe-MCM-41 s are shown in Fig. 1. The BET surface area, pore size and pore volume of the prepared materials are compiled in Table 1. The three samples show a type-IV isotherm, which is a typical feature of mesoporous structure. The pure mesoporous silica support MCM-41 shows high BET surface area (898.82 m^2/g) and pore volume (0.91 cm^3/g), which obviously decrease in the cases of 2Fe-MCM-41 and 4Fe-MCM-41 after incorporation of iron ions in the molecular sieve framework. Pore size distribution analysis revealed that the pore sizes of all samples are predominately around 2.5 nm. The pore size of iron-doped sample is smaller than that of the pure MCM-41.

The HRTEM images of the Fe-MCM-41 with different Fe contents are shown in Fig. 2a–c. The ordered pore arrangements and parallel channels are obvious for all Fe-MCM-41 samples, and the pore sizes are nearly 2.5 nm, which is consistent with the average pore diameter measured by the BJH method. Small angle X-ray scattering measurements of Fe-MCM-41 are shown in Fig. 2d. The X-ray scattering pattern shows several sharp peaks appear at $2\theta = 2.3°$, 3.9°, 4.4° and 5.8°, corresponding to (100), (110), (200)

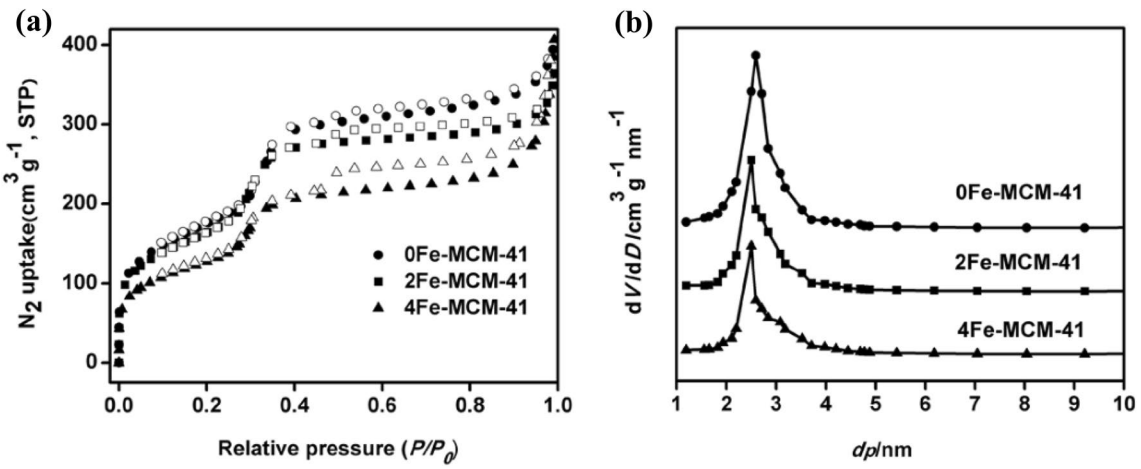

Fig. 1 **a** N_2 sorption isotherms and **b** pore size distribution of all Fe-MCM-41 samples

Table 1 Physicochemical properties of all Fe-MCM-41 samples

Sample	Surface area (m^2/g)	Pore diameter (nm)	Pore volume (cm^3/g)	Amount of acid (mmol/g)			Fe/Si (%)
				Weak	Medium	Total	
0Fe-MCM-41	898.82	2.63	0.91	0.04	0.02	0.06	0.0
2Fe-MCM-41	653.78	2.53	0.88	0.16	0.22	0.38	1.9
4Fe-MCM-41	640.94	2.48	0.87	0.16	0.30	0.46	3.8

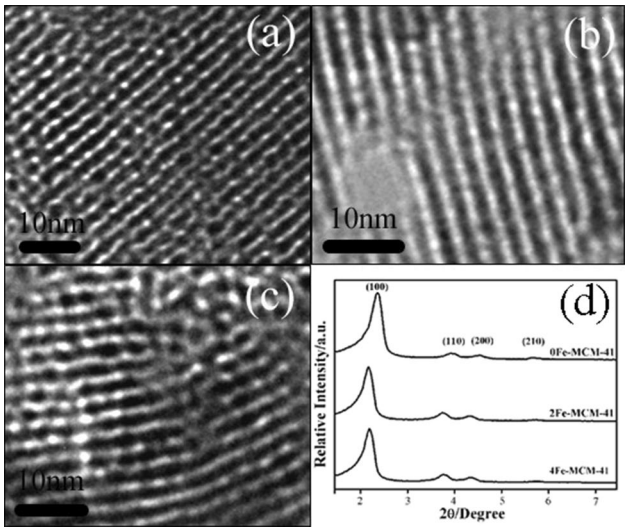

Fig. 2 HRTEM images of **a** 0Fe-MCM-41, **b** 2Fe-MCM-41 and **c** 4Fe-MCM-41; **d** small-angle XRD pattern of all Fe-MCM-41 samples

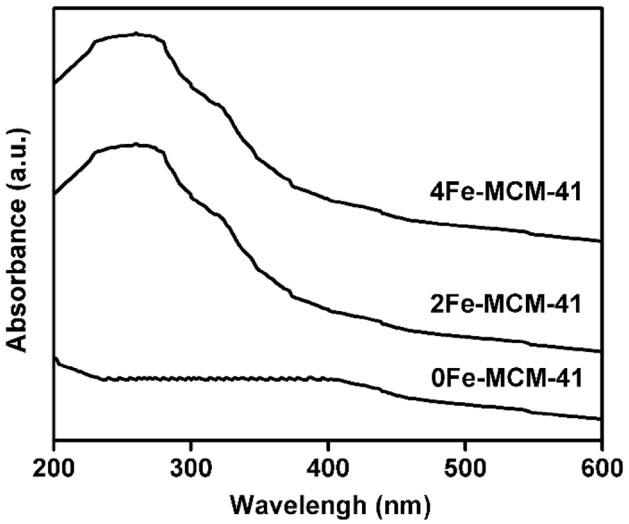

Fig. 3 UV–Vis spectra of all Fe-MCM-41 samples

and (210) reflections of pure MCM-41 respectively. This phenomenon indicates that the Fe-MCM-41 synthesized under hydrothermal conditions has high crystallinity and the regular mesoporous structures are well preserved. However, the introduction of Fe content cause the main sharp peak of Fe-MCM-41 corresponding to (100) reflection shifting to the lower angle region. This is because the atom radius of Fe is larger than the Si, so that the unit cell becomes larger after the Fe species enter the framework. Furthermore, as the iron content increases, the structural regularity of the samples also decreases, which can be seen from the weaker diffraction peaks in the range of 3°–7°.

Figure 3 shows the diffuse reflectance UV–Vis spectra of the Fe-MCM-41 materials with different Fe contents. A broad band is observed at 260 nm, which indicates the presence of iron in tetrahedral coordination geometry and proves the Fe are covalently bonded to the network of MCM-41 [25]. On the other hand, no peaks at 385 and 510 nm attributed to the Fe_2O_3 are observed, indicating no bulk crystal of Fe_2O_3 is formed. The bulk Fe/Si molar ratio of samples were measured by ICP, and are listed in Table 1. The results show that the measured data is basically consistent with the theory value, suggesting that most iron species are inserted into the molecular sieve framework.

The FT-IR spectra of the representative Fe-MCM-41 are shown in Fig. 4 in the wavenumber region of 400–2000 cm^{-1}. The bands at 804 and 1086 cm^{-1} are assigned to the symmetric and asymmetric stretching vibration of the tetrahedral SiO_4 units respectively. Moreover, the band at 1636 cm^{-1} is assigned to the stretching vibration of surface Si–OH group and another band at 463 cm^{-1} is ascribed to symmetrical Si–O vibration. The band at 960 cm^{-1} is attributed to Si–O–Fe vibration in the Fe-silicate, which can be the possible evidence of the isomorphous substitution of Si atom by Fe atom [26].

The acid properties of Fe-MCM-41 were characterized by NH_3-TPD (Table 1; Fig. 5). According to NH_3 desorption energy measurements, the signals in the 180–250, 250–380 and 380–500 °C region are assigned to weak, medium and strong Lewis acid sites, respectively [27]. It is noticeable that MCM-41 shows mainly weak acidity, with only a small amount of medium acidity. However, after the iron is doped into the silica matrix, the acidity, especially the acid center of the prepared Fe-MCM-41, has been obviously improved. Therefore, it is expected that the catalytic activity should be better than that of MCM-41 used as catalysts in the

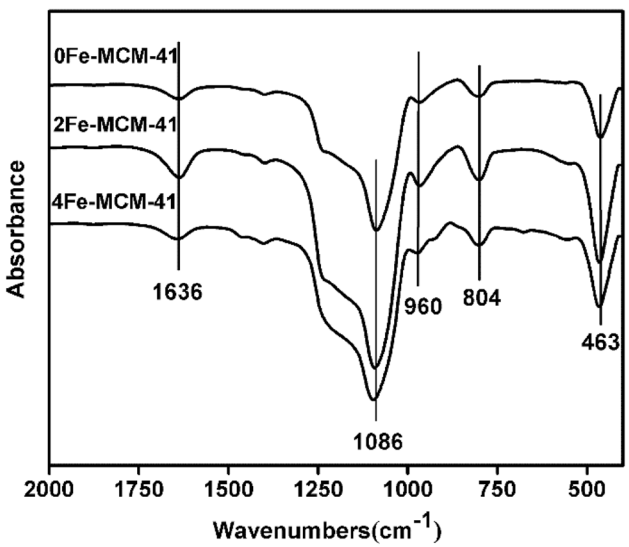

Fig. 4 FT-IR spectra of all Fe-MCM-41 samples

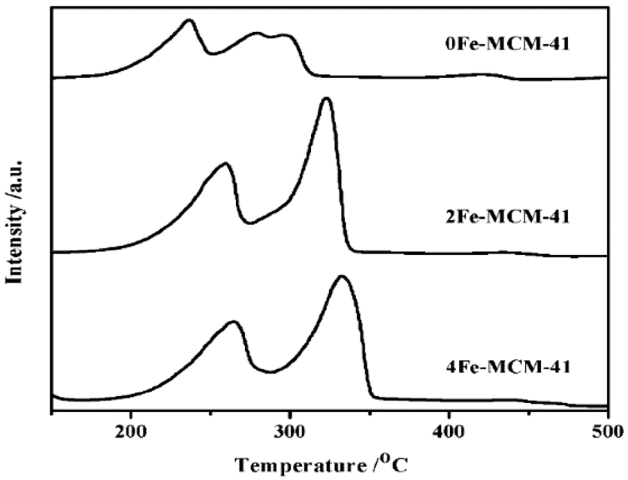

Fig. 5 NH_3-TPD of Fe-MCM-41 samples

acidolysis reaction of benzyl chloride with pivalic acid. The amount of NH_3 desorbed from each sample is summarized in Table 1. Compared to 0Fe-MCM-41 with slight amount of acid sites, the Fe doped samples show an obviously increase in acid amount, and the amount of NH_3 in the desorption process increases with the improvement of the Fe content. On the other hand, this phenomenon also indicates that Fe^{3+} has entered the molecular sieve framework and replaces Si^{4+} in the molecular sieve, which reduces the charge of molecular sieve. As a result, the prepared Fe-MCM-41 has greater acidity.

3.2 Catalytic performance

3.2.1 Catalysts screening

The catalytic performance of different catalysts in the acidolysis reaction of benzyl chloride with pivalic acid to produce benzaldehyde and pivaloyl chloride is shown in Table 2. We firstly compare the catalytic activity of homogeneous acid catalysts with the solid acid catalysts. The homogeneous catalysts, $FeCl_3$, $SnCl_4$, $AlCl_3$ and $ZnCl_2$, exhibit high catalytic activity and selectivity. Although the amount of 4Fe-MCM-41 used in this reaction is only a tenth of $FeCl_3$, the yield of benzaldehyde and pivaloyl chloride reach up to 95.5 and 95.1% respectively, which is even better than $FeCl_3$. However, the yield of benzaldehyde and pivaloyl chloride over 0Fe-MCM-41 is only 49.4 and 49.1% respectively. The exceptional catalytic performance of 4Fe-MCM-41 is related to the improved acid intensity and acid amount of the the Fe doped samples Fe-MCM-41. Moreover, the catalytic activities of the Sn-MCM-41, Zn-MCM-41 and Al-MCM-41 also exhibit good catalytic activity, but they are much lower than 4Fe-MCM-41. Therefore, we choose 4Fe-MCM-41 for further investigation.

Table 2 The acidolysis reaction of benzyl chloride with pivalic acid over different catalysts

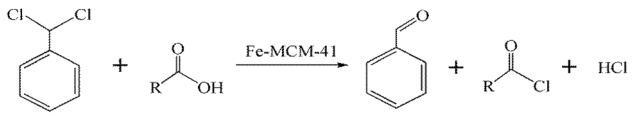

Entry	Catalyst[a]	Catalyst loading (%)[b]	Conversion of fatty acid (%)	Selectivity		Yield		Catalytic activity (g/g)[c]
				Aldehyde	Pivaloyl chloride	Aldehyde	Pivaloyl chloride	
1	$SnCl_4$	0.5	93.7	99.0	98.1	92.8	91.9	0.75
2	$ZnCl_2$	0.5	91.0	97.9	98.4	89.1	89.5	0.73
3	$FeCl_3$	0.5	95.0	98.5	98.9	93.5	94.0	0.76
4	$AlCl_3$	0.5	90.4	98.6	99.3	89.1	89.8	0.72
5	MCM-41	0.04	49.8	99.1	98.6	49.4	49.1	5.01
6	4Fe-MCM-41	0.04	96.8	98.7	98.2	95.5	95.1	9.73
7	4Sn-MCM-41	0.04	75.9	98.1	99.6	74.5	75.6	7.62
8	4Zn-MCM-41	0.04	71.7	98.8	98.6	70.8	70.7	7.20
9	4Al-MCM-41	0.04	69.3	99.2	98.5	68.7	68.3	6.96

[a]Reaction conditions: the reaction temperature is 110 °C, molar ratio of benzal chloride to fatty acid is 2, reaction time is 1 h

[b]Mass ratio of the catalyst to the reactants

[c]The converted acid mass over unit mass of catalyst per minute

3.2.2 Effect of the catalyst loading

We varied the catalyst amount within the range of 0.00–0.06% mass ratio of reactants to explore the optimal catalyst amount for the reaction. As shown in Fig. 6, the conversion of pivalic acid increases gradually with the increase of the amount of catalyst. The conversion of pivalic acid was only 45.5% without using any catalyst. When the catalyst amount increased to 0.04%, the conversion of pivalic acid reaches a maximum of 97.6% and selectivity of benzaldehyde and pivaloyl chloride is up to 99.3 and 98.7% respectively. However, when the catalyst amount furtherly increased from 0.04 to 0.06%, the conversion of pivalic acid does not change significantly, which may be attributed to the saturation of the active Lewis acid sites in the reaction solution.

3.2.3 Effect of the iron content

The influence of the iron content of the catalyst on the conversion of pivalic acid is examined by changing the molar ratio of Fe/Si from 0 to 8%. As shown in Fig. 7, all samples exhibit very high selectivity of benzaldehyde and pivaloyl chloride. When the molar ratio of Fe/Si increase from 0 to 4%, the conversion of pivalic acid increases from 49.8 to 97.6%. However, further increase in the molar ratio of Fe/Si contributed less to the increase of conversion. With the increase of Fe content, the catalyst can provide more acid sites, accelerate the reaction rate, and rapidly increase the conversion of pivalic acid. However, when the doping amount of Fe exceeds 4%, the catalytic activity remains unchanged. The reason is that the excessive Fe is less likely to enter the framework of the MCM-41 and thereby restrain the generation of more acid sites. This

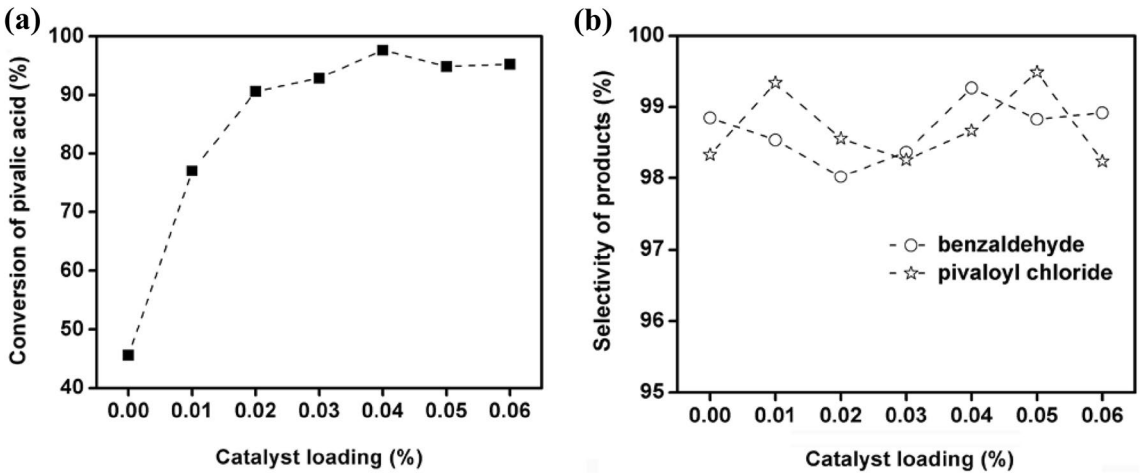

Fig. 6 **a** The conversion of pivalic acid and **b** the selectivity of benzaldehyde and pivaloyl chloride under different catalyst loadings

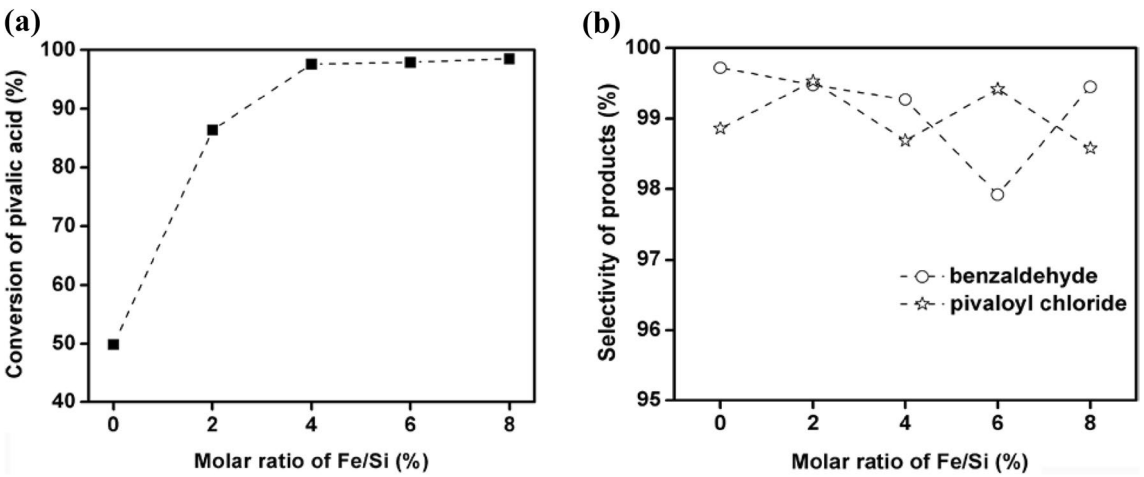

Fig. 7 **a** The conversion of pivalic acid and **b** the selectivity of benzaldehyde and pivaloyl chloride over catalysts with different iron contents

phenomenon furtherly demonstrate that the Fe content directly affects the acid strength of the Fe-MCM-41, and Fe species are the active centers of the reaction.

3.2.4 Effect of the molar ratio between starting materials

The molar ratio of benzyl chloride to pivalic acid is an important parameter that affects the conversion of pivalic acid. As can be seen from Fig. 8, the conversion of pivalic acid increased distinctly as the molar ratio of benzyl chloride to pivalic acid was raised from 1:1 to 1.6:1. However, it seems that the conversion of pivalic acid reached a maximum value of 97.6% when the molar ratio was 1.6:1. Therefore, the optimum molar ratio of benzyl chloride to pivalic acid was 1.6:1.

3.2.5 Effect of the reaction temperature

Figure 9 shows the influence of the reaction temperature for acidolysis reaction of benzyl chloride with pivalic acid. The experiments were conducted using 0.04 wt% 4Fe-MCM-41 of reaction solution, 1.6:1 of molar ratio between benzyl chloride and pivalic acid at different temperatures (80, 90, 100,110 and 120 °C). With the increase of reaction temperature from 80 to 110 °C, the conversion of pivalic acid increases progressively. However, no significant increase of conversion is observed when temperature increase from 110 to 120 °C. Therefore, the optimal reaction temperature for the acidolysis reaction of benzyl chloride with pivalic acid is 110 °C, at which we obtain a high conversion of up to 97.6%.

We then extend the scope of fatty acids in this coproduction reaction. The molar ratio of benzyl chloride/fatty acid was 1.6, the reaction temperature is 110 °C, and the catalyst

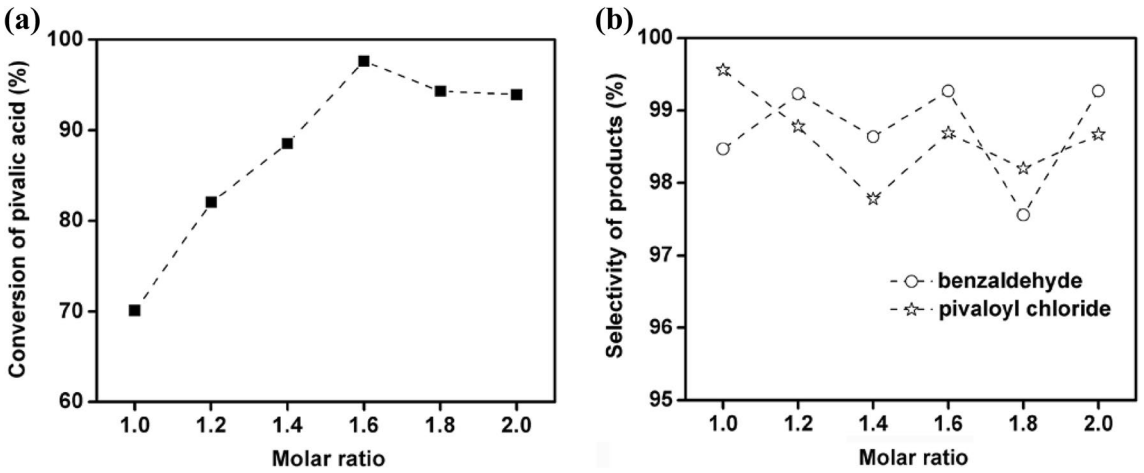

Fig. 8 **a** The conversion of pivalic acid and **b** the selectivity of benzaldehyde and pivaloyl chloride with different molar ratio of raw materials

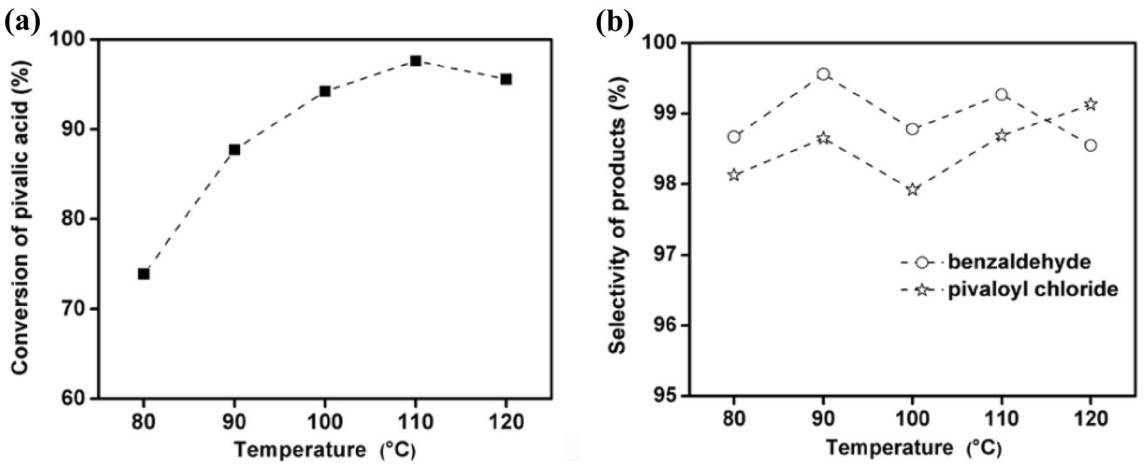

Fig. 9 **a** The conversion of pivalic acid and **b** the selectivity of benzaldehyde and pivaloyl chloride under different reaction temperatures

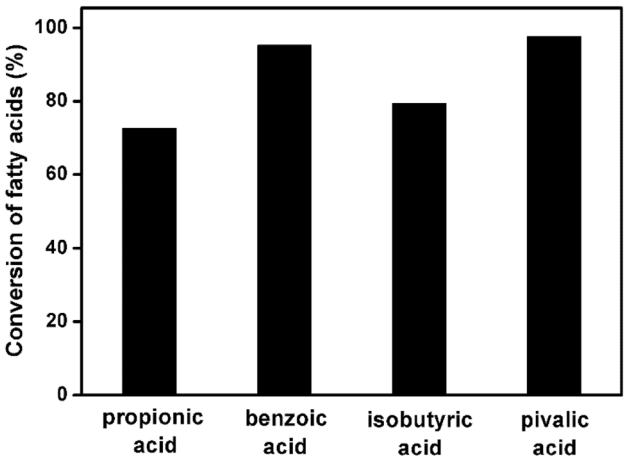

Fig. 10 4Fe-MCM-41 catalytic benzyl chloride with various acid

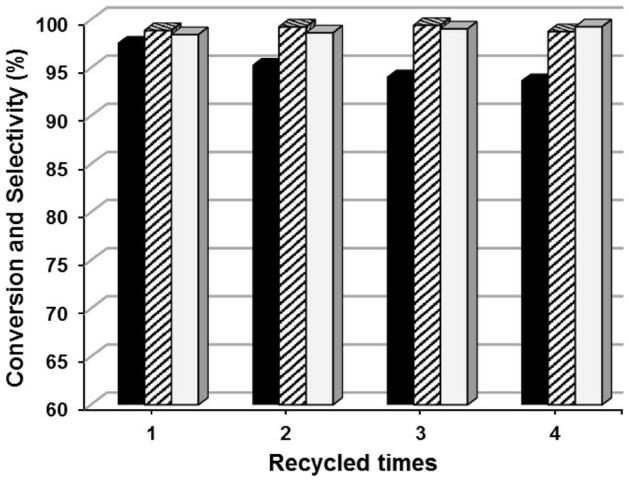

Fig. 11 Conversion of pivalic acid (black column) and selectivity of benzaldehyde (striated column) and pivaloyl chloride (white column) during four reaction cycles of 4Fe-MCM-41

amount is 0.04 wt% of the reaction solution. As is seen in Fig. 10, the 4Fe-MCM-41 also shows excellent catalytic performance for other fatty acids, including propionic acid, benzoic acid and isobutyric acid, which indicates that the Fe-MCM-41 is a universal catalyst for the acidolysis reaction of benzyl chloride with varieties of fatty acids.

3.2.6 Reusability of catalyst

To investigate the reusability of 4Fe-MCM-41, the catalyst was collected and re-activated at 150 °C under vacuum overnight before starting a new cycle. Catalytic activity for each run is summarized in Fig. 11. There is a minor reduction of the conversion of pivalic acid from 97.6% (fresh) to 93.5% (4th run), but the selectivity of benzaldehyde and pivaloyl chloride for all recycled runs remains almost the same.

4 Conclusion

In summary, the heterogeneous Lewis acid catalyst Fe-MCM-41 with different Fe contents are synthesized via direct hydrothermal method. According to XRD and N_2 adsorption–desorption characterization results, the Fe-doped mesoporous silica has a large specific surface area and pore volume, and maintains the highly ordered mesoporous structure of the pure MCM-41. FT-IR and UV–Vis results indicate that the iron species have entered the mesoporous silica framework and Fe^{3+} has replaced Si^{4+} in mesoporous silica, which reduces the charge of mesoporous silica. As a result, the total acid amount of the prepared 4Fe-MCM-41 increase from 0.06 to 0.46 mmol/g compared with the pure MCM-41, which is confirmed by the NH_3-TPD results. Finally, the result of catalyst investigation shows that the prepared 4Fe-MCM-41 exhibit high catalytic activity for the acidolysis reaction of benzyl chloride with various fatty acids.

Acknowledgements The author gratefully acknowledges the financial support from National Key R&D Program of China (2017YFB0307304), National Natural Science Foundation of China (21676141, 21606130), Natural Science Foundation of Jiangsu Province (BK20170989), Natural Science Foundation of Jiangsu Higher Education Institutions of China (17KJB530005), Six Major Talent Peak Project of Jiangsu Province (XCL-017) and Project "333" of Jiangsu Province (BRA2016418).

References

1. A. Corma, H. García, Chem. Rev. **103**, 4307–4366 (2003)
2. D.W. Stephan, Acc. Chem. Res. **48**, 306–316 (2015)
3. P.Y. Dapsens, C. Mondelli, J. Perez-Ramirez, Chem. Soc. Rev. **44**, 7025–7043 (2015)
4. P.T. Anastas, M.M. Kirchhoff, Acc. Chem. Res. **35**, 686–694 (2002)
5. A.H. Chughtai, N. Ahmad, H.A. Younus, A. Laypkov, F. Verpoort, Chem. Soc. Rev. **44**, 6804–6849 (2015)
6. P. Ferrini, J. Dijkmans, R. De Clercq, S. Van de Vyver, M. Dusselier, P.A. Jacobs, B.F. Sels, Coord. Chem. Rev. **343**, 220–255 (2017)
7. J. Sudhakar Reddy, R. Kumar, J. Catal. **130**, 440–446 (1991)
8. G. Ferey, C. Mellot-Draznieks, C. Serre, F. Millange, J. Dutour, S. Surble, I. Margiolaki, Science **309**, 2040–2042 (2005)
9. C. Serre, F. Millange, C. Thouvenot, M. Nogues, G. Marsolier, D. Louer, G. Ferey, J. Am. Chem. Soc. **124**, 13519–13526 (2002)
10. J.C. Jiang, F. Gandara, Y.B. Zhang, K. Na, O.M. Yaghi, W.G. Klemperer, J. Am. Chem. Soc. **136**, 12844–12847 (2014)
11. M. Kandiah, M.H. Nilsen, S. Usseglio, S. Jakobsen, U. Olsbye, M. Tilset, C. Larabi, E.A. Quadrelli, F. Bonino, K.P. Lillerud, Chem. Mater. **22**, 6632–6640 (2010)
12. H. Zhou, Y.M. Wang, W.Z. Zhang, J.P. Qu, X.B. Lu, Green Chem. **13**, 644–650 (2011)
13. P. Devi, U. Das, A.K. Dalai, Chem. Eng. J. **346**, 477–488 (2018)

14. K. Soni, B.S. Rana, A.K. Sinha, A. Bhaumik, M. Nandi, M. Kumar, G.M. Dhar, Appl. Catal. B **90**, 55–63 (2009)
15. M. Xia, M.C. Long, Y.D. Yang, C. Chen, W.M. Cai, B.X. Zhou, Appl. Catal. B **110**, 118–125 (2011)
16. X.B. Ma, H.W. Chi, H.R. Yue, Y.J. Zhao, Y. Xu, J. Lv, S.P. Wang, J.L. Gong, AIChE J. **59**, 2530–2539 (2013)
17. B.Y. Lan, R.H. Huang, L.S. Li, H.H. Yan, G.Z. Liao, X. Wang, Q.Y. Zhang, Chem. Eng. J. **219**, 346–354 (2013)
18. A.I. Carrillo, E. Serrano, J.C. Serrano-Ruiz, R. Luque, J. Garcia-Martinez, Appl. Catal. A **435**, 1–9 (2012)
19. X. Chu, D. Zhou, D. Li, K. Xia, N. Gan, X.H. Lu, R.F. Nie, Q.H. Xia, Microporous Mesoporous Mater. **230**, 166–176 (2016)
20. E.G. Vaschetto, G.A. Monti, E.R. Herrero, S.G. Casuscelli, G.A. Eimer, Appl. Catal. A **453**, 391–402 (2013)
21. Y.Q. Jiang, K.F. Lin, Y.N. Zhang, J. Liu, G.H. Li, J.M. Sun, X.Z. Xu, Appl. Catal. A **445**, 172–179 (2012)
22. W. Xu, T. Ollevier, F. Kleitz, ACS Catal. **8**, 1932–1944 (2018)
23. C. Ruppin, P. Corbiere, EU Patent EP926125A1, 1999
24. S.K. Badamali, P. Selvam, Catal. Today **141**, 103–108 (2009)
25. Y. Wang, Q.H. Zhang, T. Shishido, K. Takehira, J. Catal. **209**, 186–196 (2002)
26. T.K. Das, K. Chaudhari, A.J. Chandwadkar, S. Sivasanker, J. Chem. Soc. Chem. Commun. **24**, 2495–2496 (1995)
27. V.R. Choudhary, K. Mantri, Langmuir **16**, 8024–8030 (2000)